

A probabilistic approach to the N-body problem

M. Romero¹ and Y. Ascasibar^{1,2}

¹ *Departamento de Física Teórica, Universidad Autónoma de Madrid, Madrid 28049, Spain*

² *Astro-UAM, UAM, Unidad Asociada CSIC*

17 March 2017

ABSTRACT

This work introduces a new interpretation of the gravitational N-body problem, based on the one-point probability density Ψ of finding a particle at a given location of phase space (x, v) at time t and the associated *expected* phase-space density $\bar{f}(x, v, t) = M\Psi(x, v, t)$, where M is the total mass of the system. At variance with the traditional paradigm, we consider that the problem is inherently stochastic, and therefore \bar{f} corresponds to a weighted average over all possible random realisations of the initial conditions. In practice, we run several numerical experiments in one dimension where $\bar{f}(x, v, t)$, and thus $\Psi(x, v, t)$, are estimated from the average of a finite number S of independent simulations with N particles each. The proposed approach is extremely efficient from a computational point of view, with modest CPU and memory requirements, and it provides a very competitive alternative to traditional N-body simulations when the goal is to study the average properties of N-body systems, at the cost of abandoning the notion of well-defined trajectories for each individual particle.

Key words: gravitation - methods: numerical - galaxies: kinematics and dynamics - galaxies: statistics

1 INTRODUCTION

At large scales, almost all interactions in the Universe are dominated by gravity. Nuclear forces are short-range, and, as far as electromagnetism is concerned, there seem to be, on average, the same amount of positive and negative charges. Most of the processes studied in Astrophysics and Cosmology involve, one way or another, a set of objects (planets, stars, galaxies...) that interact with each other through their mutual gravitational attraction. More specifically, the N-body problem refers to the evolution of a self-gravitating system formed by N point-like particles, and its solution is of vital importance in many contexts, from gravitational instability (e.g. planet, star or galaxy formation) to the dynamics of systems in equilibrium (which determines the internal properties of planetary systems, star clusters, galaxies, galaxy clusters...).

Writing the equations of motion for an N-body system is easy, but solving them is not. Analytical solutions are only known for $N = 2$ and some particular conditions with $N = 3$. Thus, in most applications of interest in Astrophysics, the equations are solved numerically, using a set of initial conditions and studying the evolution of the system in time. When N is small, the mutual interactions between particles can be evaluated directly, and the main source of uncertainty is the numerical integration error. Nevertheless, the number of force evaluations grows as N^2 , and the direct method quickly becomes impractical. Using hybrid paralleli-

sation techniques in specialized (CPU+GPU) hardware, the maximum number of particles that can be dealt by direct integration is of the order of one million (Wang et al. 2015).

For larger values of N , it is necessary to use approximations that reduce the number of force evaluations. For example, by computing the accelerations from close neighbours directly, whereas the interaction between groups of particles far away are obtained from their mass moments. Many of these algorithms use a tree structure to choose what particles are close and which are not, hence the number of evaluations scales as $N \log(N)$ (Barnes & Hut 1986) or even close to N (Dehnen 2000). For the reader interested in this particular topic, see e.g. Aarseth (2003).

In many cases, though, the number of objects to simulate in a real system is much greater than the number of particles that the best supercomputers can handle. The Milky Way, for example, contains approximately 10^{11} stars and about $10^{12} M_{\odot}/m_{dm}$ particles of dark matter with mass m_{dm} (Binney & Tremaine 2008), and thus it is virtually impossible to simulate every one of them individually. When the number of particles is so large, one usually relies on the long-range character of the gravitational interaction to make an important approximation: the gravitational acceleration of any particle is not dominated by its nearest neighbours, but by the mean potential created by the global density distribution. Under these conditions (i.e. in the limit $N \rightarrow \infty$), it is assumed that the system is fully described by a contin-

uous *distribution function*

$$f(\mathbf{x}, \mathbf{v}) \equiv \frac{dM}{d^3\mathbf{x} d^3\mathbf{v}} \quad (1)$$

that indicates the density in phase space (i.e. the amount of mass located at position \mathbf{x} moving with velocity \mathbf{v} per unit of six-dimensional volume $d^3\mathbf{x} d^3\mathbf{v}$).

Given the distribution function, the mass density at any spatial location \mathbf{x} can be obtained by integrating over all possible velocities

$$\rho(\mathbf{x}) \equiv \int_{-\infty}^{\infty} f(\mathbf{x}, \mathbf{v}) d^3v \quad (2)$$

whereas integration over configuration space (the three-dimensional spatial volume) yields the velocity distribution of the system

$$\eta(\mathbf{v}) \equiv \int_{-\infty}^{\infty} f(\mathbf{x}, \mathbf{v}) d^3x \quad (3)$$

The temporal evolution of the distribution function is given by the collisionless Boltzmann equation

$$\frac{df}{dt} = \frac{\partial f}{\partial t} + \mathbf{v} \frac{\partial f}{\partial \mathbf{x}} + \mathbf{a} \frac{\partial f}{\partial \mathbf{v}} = 0 \quad (4)$$

which is nothing other than Liouville's theorem (density conservation in phase space), where $\mathbf{a}(\mathbf{x})$ corresponds to the acceleration associated to the Newtonian gravitational potential¹.

Traditionally, it is considered that equation (4) provides a valid approximation to the dynamics of a *finite* N-body system as long as the individual interactions between two or more particles may be neglected. The range of validity is usually expressed in terms of the relaxation time

$$t_{\text{relax}} \approx 0.1 \frac{N}{\ln(N)} t_{\text{char}} \quad (5)$$

where t_{char} denotes the time it takes for a particle to cross (or take half an orbit around) the system. The relaxation time t_{relax} is also meant to provide an idea of the time it takes a particle to randomize its velocity due to individual encounters (collisions) with other bodies and lose all memory of its initial conditions. The exact value of t_{relax} varies greatly depending on the local density and the total number of particles. For the stars in the Milky Way, $N \sim 10^{11}$ and $t_{\text{char}} \sim 0.1$ Gyr; t_{relax} is much longer than the age of the Universe, and therefore (4) is considered a good approximation. On the other hand, for globular ($t_{\text{char}} \sim 0.1$ Myr, $N \sim 10^5$) and open ($t_{\text{char}} \sim 1$ Myr, $N \sim 100$) clusters, $t_{\text{relax}} \sim 87$ and 2 Myr, respectively, and two-body encounters play an important role in the evolution of the distribution function (Binney & Tremaine 2008).

When N is small (and/or t_{relax} is smaller than the time scales of interest), interactions are simulated directly. When $N \rightarrow \infty$ and $t_{\text{relax}} \rightarrow \infty$, equation (4) can be integrated in many ways (see e.g. Colombi & Touma 2014; Mocz & Succi 2017, and references therein, for a comparison of different methods), but a lot of them rely on sampling the distribution function, assumed to be approximately continuous,

with a finite number of tracers, $N' \ll N$, that represent a certain amount of mass. The continuous function $f(x, v, t)$ is approximated by means of these tracers, interacting with each other through their mutual gravity, with some kind of small-scale filtering to prevent two-body interactions (because they no longer represent point-like masses, as in the direct case; see e.g. Dehnen 2001, for an in-depth discussion of this 'gravitational softening'). It is (implicitly or explicitly) assumed that, the higher the number of tracers used, the more the solution will resemble (4), reaching it asymptotically as $N' \rightarrow \infty$.

The main aim of the present work is to present a new interpretation of the N-body problem. In practice, it is often not important to know exactly the positions and velocities of all particles², but only the average statistical properties of the distribution function. For this reason, we propose a probabilistic approach, where the fundamental quantity is the *expected* phase-space density $\bar{f}(x, v, t)$ given by the one-point *probability density* $\Psi(\mathbf{x}, \mathbf{v}, t)$ of finding a particle with coordinates (\mathbf{x}, \mathbf{v}) at time t . We are only interested in the evolution of this function, and *not* on the trajectories of individual particles, whose coordinates at any time – including $t = 0$ – are assumed to be N statistically-independent *random* realisations of $\Psi(\mathbf{x}, \mathbf{v}, t)$, at variance with the traditional, deterministic formulation of the problem.

The evolution of such an intrinsically stochastic N-body system, fully specified by the initial condition $\Psi(\mathbf{x}, \mathbf{v}, 0)$, will be estimated by averaging over several N-body simulations, and the results will be compared with the collisionless Boltzmann equation (4) and the traditional N-body approach of approximating it using $N' \leq N$ tracers. While a similar averaging has been carried out in some previous studies (e.g. Joyce & Worrakitpoonpon 2010) on purely practical grounds, we would like to propose here a rigorous justification for such procedure and advocate for its validity in the general case (including e.g. cosmological numerical simulations), providing the formal mathematical definitions and conceptual framework that are necessary for a sound physical interpretation.

We will first discuss the distribution function and the collisionless Boltzmann equation in more detail, including some analytical solutions, in Section 2. The main aspects of our probabilistic approach are then presented in Section 3, highlighting the similarities and differences between f and \bar{f} . The evolution of the probability density Ψ is investigated by a series of numerical experiments, described in Section 4. The main results are shown in Section 5, and they are compared with the traditional approach in Section 6. Our conclusions are briefly summarized in Section 7.

2 ANALYTICAL SOLUTIONS FOR THE DISTRIBUTION FUNCTION

Let us start by considering the evolution of a truly continuous fluid in phase-space, stressing that this is *different* from an N-body system, even as $N \rightarrow \infty$ (see below). For the

¹ In this case, expression (4) is also called Vlasov-Poisson equation (see Henon 1982, for a discussion of the optimal nomenclature).

² Something that can hardly be achieved in a traditional N-body simulation anyway, due to the approximations involved in the force evaluation.

sake of simplicity, as well as computational accuracy and efficiency, we will work in one spatial dimension, but all our results can be readily extrapolated to the three-dimensional case. The Poisson equation

$$\frac{\partial^2 \phi(x)}{\partial x^2} = 2\pi G \rho(x) \quad (6)$$

implies that the gravitational potential at any spatial location x is given by the expression

$$\phi(x) = 2\pi G \int_{-\infty}^{\infty} \rho(x') |x - x'| dx' \quad (7)$$

and the gravitational acceleration that appears in the collisionless Boltzmann equation

$$a(x) = 2\pi G \left[\int_x^{\infty} \rho(x') dx' - \int_{-\infty}^x \rho(x') dx' \right] \quad (8)$$

is just proportional to the difference between the amount of mass to the right and the left of x .

Equations (4) and (8) provide an *exact* description of the evolution of the distribution function $f(x, v, t)$ for a continuous one-dimensional fluid. In general, it is necessary to solve these equations by numerical integration, but analytical solutions may be found for some particular sets of initial conditions. Here we will make use of two such solutions to illustrate the similarities and differences between the distribution function f and the probability density Ψ .

For a discrete distribution of N point-like particles with equal mass m , the phase-space density is a sum of Dirac delta functions

$$f(x, v, t) = m \sum_{i=1}^N \delta(x - x_i(t)) \delta(v - v_i(t)) \quad (9)$$

and the gravitational acceleration can be expressed as

$$a(x) = 2\pi G m [N_+(x) - N_-(x)] \quad (10)$$

where N_+ and N_- denote the number of particles to the right and left of x , respectively.

Although equation (9) will never become a continuous function, no matter how large N may be, all of the considerations above regarding continuous fluids still hold. In particular, the evolution of $f(x, v, t)$ is *exactly* determined by the Vlasov-Poisson equation at all times. It is only when one introduces some (often loosely defined) smoothing in order to obtain a finite and continuous ‘coarse-grained’ distribution function, that equation (4) becomes an approximation. Finding an analytic solution for a system of N particles is even more difficult than for the continuous fluid, but, once again, it is possible for very specific initial conditions.

Finally, let us note that one of the most common examples of smoothing is the tracer-based approach to N -body simulations, where the distribution function is approximated by the sum

$$f'(x, v, t) = m' \sum_{i=1}^{N'} K(x - x_i(t)) \delta(v - v_i(t)) \quad (11)$$

where m' is the mass of the N' tracer particles and $K(x)$ is the gravitational softening kernel. In this case the evolution of f' is usually followed by updating the positions x_i and velocities v_i of the tracers, and therefore it resembles, but it does *not* exactly correspond to equation (4). While

this quantity is undoubtedly interesting in its own right, it deviates from our main goal, and it will not be investigated further.

2.1 Stationary solutions

It is easy to show (see e.g. [Binney & Tremaine 2008](#)) that any distribution function of the form $f(\epsilon)$, where $\epsilon = \frac{v^2}{2} + \phi(x)$ denotes the energy per unit of mass of a particle located at (x, v) , is a stationary solution of the collisionless Boltzmann equation:

$$\begin{aligned} \frac{\partial f}{\partial t} + v \frac{\partial f}{\partial x} + a \frac{\partial f}{\partial v} &= \frac{\partial f}{\partial t} + v \frac{\partial \phi}{\partial x} \frac{\partial f}{\partial \epsilon} - v \frac{\partial \phi}{\partial x} \frac{\partial f}{\partial \epsilon} = \\ &= \frac{\partial f}{\partial t} = 0 \end{aligned} \quad (12)$$

In principle, one may expect that, on time scales much longer than t_{relax} , collisions would eventually drive the system towards one such state, subject to the conservation of total mass and energy. Other (collisionless) processes, collectively known as ‘violent relaxation’ ([Lynden-Bell 1967](#)) may achieve a similar effect on much shorter time scales, and several authors (e.g. [Ogorodnikov 1957](#); [Lynden-Bell 1967](#); [Shu 1978](#); [Plastino & Plastino 1993](#); [Hjorth & Williams 2010](#), among others) have tried to derive the precise function $f(\epsilon)$ from statistical mechanics arguments (e.g. by maximising a suitably-defined entropy). These quasi-stationary states are out of equilibrium, and it is expected that, after a sufficiently long time (that increases with particle number), collisions will drive them towards thermal equilibrium (see e.g. [Rybicki 1971](#); [Joyce & Worrakitpoonpon 2010](#); [Levin et al. 2014](#), and references therein).

Of course, strictly stationary solutions are *not* possible for any natural number N , for the simple reason that (9) can only adopt the form $f(\epsilon)$ in the trivial case $x_i = v_i = 0$ for every particle i . For any other configuration, a discrete system composed of N point-like particles can *never* be stationary in the sense of $\frac{\partial f}{\partial t} = 0$.

2.2 Periodic solution

A simple analytic solution can be obtained for a continuous system starting at rest ($v = 0$) at $t = 0$, with uniform spatial density $\rho(x) = \frac{1}{L}$ between $x = -\frac{L}{2}$ and $x = \frac{L}{2}$:

$$f(x, v, 0) = H(x + \frac{L}{2}) H(\frac{L}{2} - x) \delta(v) \quad (13)$$

where $H(x)$ denotes the Heaviside step function.

Without loss of generality, we will choose from now on our units of mass, length, and time, so that $Nm = 1$, $L = 1$, and $2\pi G = 1$, respectively. In these units, the acceleration at the initial time is simply $a(x) = -2x$, and the system will start shrinking homologously; the velocity is proportional to x , and thus the density evolves with time, but maintaining the same (constant) form. Since there is no crossing between fluid elements, the accelerations remain constant during the collapse, and the trajectories describe a parabola in phase space

$$(x, v, t) = [x_0(1 - t^2), -2x_0 t, t] \quad (14)$$

as a function of the initial position x_0 .

This description is valid until all trajectories simultaneously reach the point $x = 0$ at $t = 1$, crossing it with velocity $v = -2x_0$. When the crossing occurs, the acceleration abruptly changes sign from $a(x, t < 1) = -2x_0$ to $a(x, t > 1) = 2x_0$. After that, the system expands until all velocities are zero again at $t = 2$, obtaining a distribution $(x, v) = (-x_0, 0)$ that is perfectly symmetrical to the original.

Summarizing, we have found a periodic solution with a characteristic crossing time $t_{\text{char}} = 2$. At any time, the system forms an infinitely-thin, straight line in phase space, and it switches between phases of expansion and contraction. At $t = (n + 1/2)t_{\text{char}}$, all points are located at $x = 0$, moving at the highest speed, whereas at $t = nt_{\text{char}}$ the distribution reaches null velocity and maximum spatial extent. Assuming that we plot x and v as the abscissa and ordinate of a phase-space diagram, respectively, the system starts as a horizontal *bar* that rotates clockwise with a period $T = 4$.

This solution is also valid for N *equispaced* particles ($x_{i+1} = x_i + \frac{1}{N-1}$) between $x_1 = -\frac{1}{2}$ and $x_N = \frac{1}{2}$. Note that, if the particles were randomly distributed (an arguably more physically-motivated, or at least infinitely more likely situation), the initial acceleration would no longer be *exactly* proportional to x_i , and thus the particles will not reach the origin at the same time. Any perturbation with respect to a perfectly *equispaced* distribution will grow in time, and the system will evolve differently depending on the precise details of the initial conditions. The particles cross each other at different times, and one may conjecture that their interactions should drive the system towards a quasi-stationary state.

3 PROBABILITY FORMULATION OF THE N-BODY PROBLEM

The main idea that we would like to put forward is that, quite often, one is not interested on the evolution of N particles with (infinitely) precisely known initial positions and velocities x_i and v_i . Instead, we would like to address the problem of N particles whose initial conditions are randomly drawn from the probability density $\Psi(x, v, 0)$. We abandon the notion of individual particle trajectories and focus on the *expected* phase-space density

$$\bar{f}(x, v, t) = Nm\Psi(x, v, t) \quad (15)$$

after time t , averaged over all possible random realisations of the initial conditions, where $\Psi(x, v, t)$ is the one-point probability density (i.e. neglecting correlations) for the distribution of particles in phase space. Although the distribution function f for any *individual* realisation of the initial conditions will be, of course, a sum of Dirac deltas, and the number of particles within a certain interval of (x, v) at time t will always be an integer number, the average density \bar{f} and the probability density Ψ will be, in general, continuous functions with real values, such that

$$\int \Psi(x, v) dx dv = 1 \quad (16)$$

at any time t . Moreover, conservation of probability can be written as

$$\frac{d\Psi}{dt} = \frac{\partial\Psi}{\partial t} + v\frac{\partial\Psi}{\partial x} + a\frac{\partial\Psi}{\partial v} = 0 \quad (17)$$

which is analogous to the collisionless Boltzmann equation, with the exception that the acceleration a is now a stochastic variable, subject to random statistical fluctuations of N_+ and N_- in (10).

Ideally, one would like to derive the precise equation that determines the evolution of Ψ and/or \bar{f} (see e.g. [Campa et al. 2009](#); [Chavanis 2013](#), and references therein, for a review of different analytical approximations). Here we adopt a more practical approach, simply aiming for an approximate solution obtained by averaging over a finite number S of independent numerical simulations with N particles each. If N does indeed correspond to the actual number of particles in the system, the limit $S \rightarrow \infty$ converges to the true solution to our probabilistic formulation of the N-body problem. Once the evolution of $\Psi(x, v, t)$ and the dependence with N are fully understood, it would be possible to quantitatively address the $N' \ll N$ case.

4 N-BODY SIMULATIONS

In order to carry out the S independent simulations to be averaged, we have developed a code that solves the N-body problem in one dimension to very high accuracy. More specifically, the trajectories of the particles are followed analytically between collisions, without any approximation, and numerical integration errors are limited to machine round-off precision (cf. [Schulz et al. 2013](#), and references therein).

We consider two different initial conditions, both with the same distribution of positions (uniform random numbers between $-\frac{1}{2}$ and $\frac{1}{2}$) but different velocity distributions. In the first initial condition, analogous to the periodic, clockwise-rotating *bar* case (13) discussed in Section 2.2, velocities are set to zero

$$\Psi(x, v, 0) = H(x + \frac{1}{2}) H(\frac{1}{2} - x) \delta(v) \quad (18)$$

whereas the other initial condition has uniform random velocities between $-\frac{1}{2}$ and $\frac{1}{2}$. In other words, the initial probability density resembles a *box* in phase space

$$\Psi(x, v, 0) = H(x + \frac{1}{2}) H(\frac{1}{2} - x) H(v + \frac{1}{2}) H(\frac{1}{2} - v) \quad (19)$$

and therefore we will refer to (18) and (19) as the *bar* and the *box* cases, respectively.

For each initial condition, we have run sets of $S = \{9000, 3000, 900\}$ simulations with $N = \{100, 300, 1000\}$ particles, so that the product $NS = 9 \times 10^5$ in all cases. With the purpose of studying the long-term evolution of the system, we consider times up to $t = 1000$, much larger than the characteristic time $t_{\text{char}} = 2$ or the relaxation time t_{relax} estimated from (5). In order to study the dependence of the results with the number of particles over a broader range in N , we have also run an additional set of $S = 50$ simulations of the *bar* case with $N = 10^6$ up to $t = 10$.

For each individual simulation, we subtract the position and velocity of the centre of mass to place the system at the origin of phase space. To measure $\Psi(x, v, t)$, we discretise the phase space in homogeneous subdivisions with $\Delta x = 0.01$ and $\Delta v = 0.01$ and evaluate the probability density at fixed values of x_i and v_j , given a set of times t_k . For a single

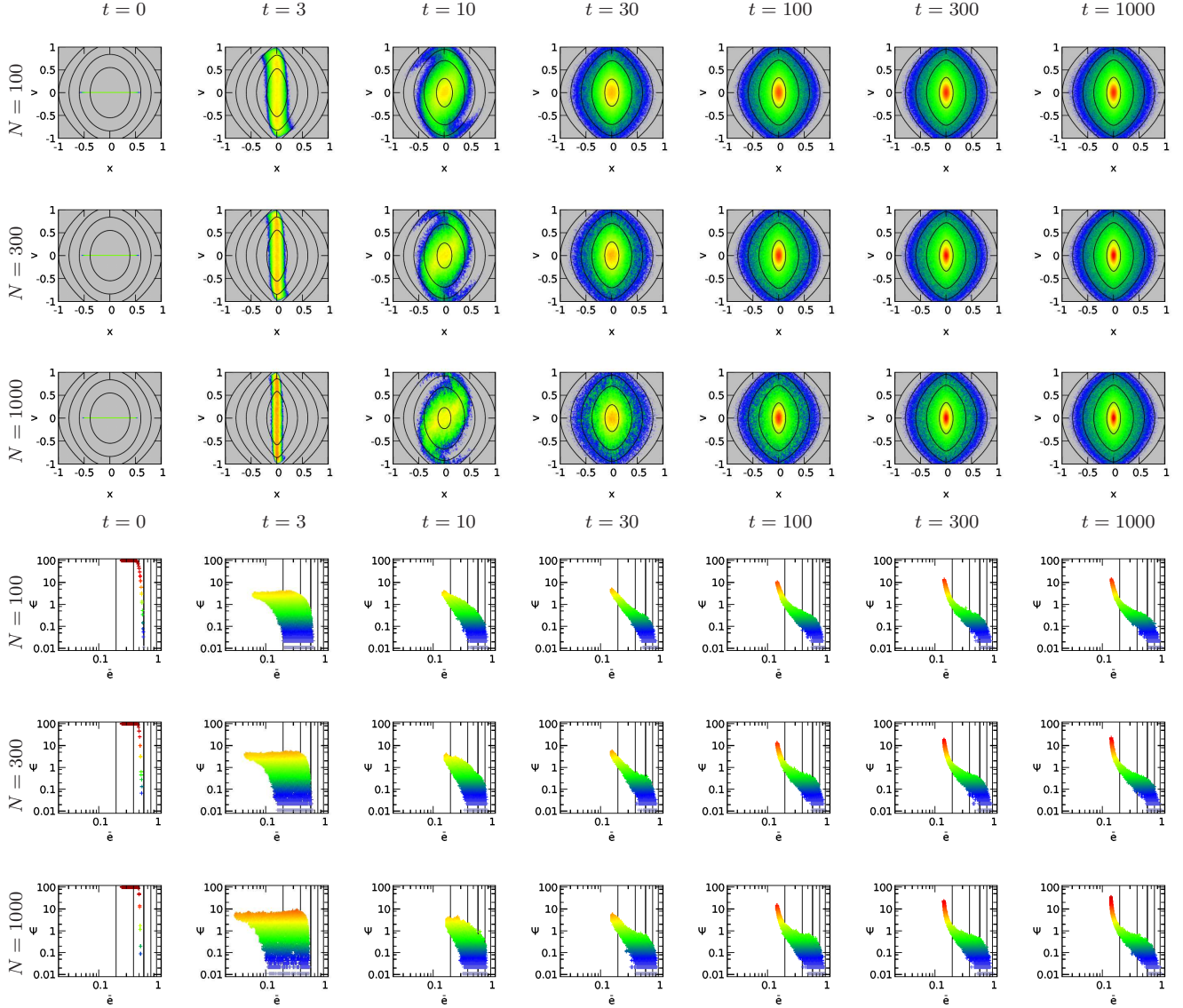


Figure 1. Top panels: evolution of the probability density $\Psi(x, v, t)$ in the *bar* case (18) for different times (columns) and number of particles (rows). Colours represent probability density (varying by about four orders of magnitude), and contours have been drawn at energies $\bar{\epsilon}(x, v) = \frac{v^2}{2} + \phi(x) = \{0.2, 0.4, 0.6, 0.8, 1.0\}$. Bottom panels: same as above, in terms of $\Psi(\bar{\epsilon})$, using identical colour scale and vertical lines to indicate energy contour levels.

simulation s , the individual probability density

$$\psi^{(s)}(x_i, v_j, t_k) \equiv \psi_{ijk}^{(s)} = \frac{n_{ijk}^{(s)}}{N \Delta x \Delta v} \quad (20)$$

is proportional to the number of particles $n_{ijk}^{(s)}$ found inside the bin $(x_i \pm \frac{\Delta x}{2}, v_j \pm \frac{\Delta v}{2})$ at time t_k . Formally, the probability density $\Psi(x, v, t)$ is given by the weighted average of all possible realisations of the initial condition. Approximating the result as an average over a finite number of simulations

$$\Psi_{ijk} = \frac{1}{S} \sum_{s=1}^S \psi_{ijk}^{(s)} \quad (21)$$

is simply a Monte Carlo method to evaluate such integral numerically. Once this quantity has been obtained, we com-

pute the mean velocity distribution

$$\bar{\eta}(v_j, t_k) \equiv \bar{\eta}_{jk} = \Delta x \sum_{i=1}^{N_x} \Psi_{ijk} \quad (22)$$

and the mean number density

$$\bar{\rho}(x_i, t_k) \equiv \bar{\rho}_{ik} = \Delta v \sum_{j=1}^{N_v} \Psi_{ijk} \quad (23)$$

where N_x and N_v correspond to the number of subdivisions in position and velocity, respectively.

5 RESULTS

Figures 1 and 2 show the evolution of the probability density Ψ at times $t = \{0, 3, 10, 30, 100, 300, 1000\}$ for

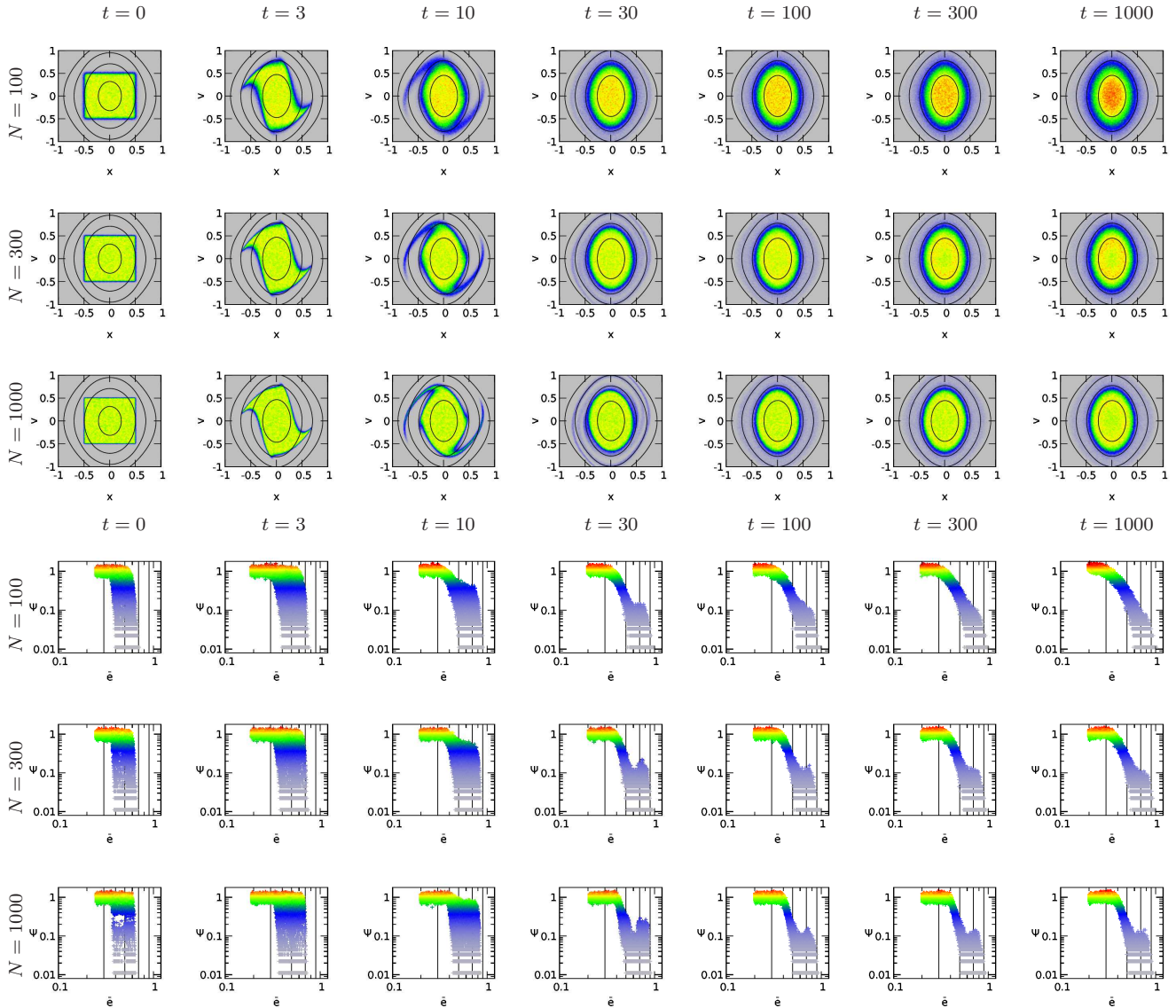


Figure 2. Same as Figure 1, for the *box* case (19). Probability density (colours) span now two orders of magnitude and energy contours have been drawn at $\bar{\epsilon} = \{0.3, 0.5, 0.7, 0.9\}$.

$N = \{100, 300, 1000\}$ in the *bar* and *box* cases, respectively. Top panels represent it as a function of the phase-space coordinates (x, v) , whereas bottom panels illustrate the dependence on the expected energy per unit of mass $\bar{\epsilon}(x, v) = \frac{v^2}{2} + \bar{\phi}(x)$. The mean density $\bar{\rho}(x)$ and the velocity distribution $\bar{\eta}(v)$ are plotted in Figures 3 and 4, respectively, for $t = \{100, 300, 1000\}$.

As anticipated in Section 3, the evolution of Ψ bears clear resemblances with the predictions of the collisionless Boltzmann equation, but also important differences. The most important is arguably a diffusion in phase space that we ascribe to the stochastic nature of the problem, which is explicitly manifest in the acceleration term in equation (17). Our results clearly show that the shape of the initial configuration is not only distorted, but also that the values of both Ψ and $\bar{\epsilon}$ are *not* strictly conserved throughout the evolution of the system. After a certain time, the combined effects of distortion (phase mixing) and (stochastic) diffusion seem

to drive the probability density towards a quasi-stationary state that admits a description of the form $\Psi(\bar{\epsilon})$. This qualitative behaviour is common to all the cases we have considered. However, there are crucial differences between the two initial conditions, as well as a certain dependence on the number of particles N .

The results obtained for our *bar* and *box* cases demonstrate that the shape of the function $\Psi(\bar{\epsilon})$ is certainly *not* universal, and it clearly retains much more memory of the initial conditions than merely the total mass and energy of the system, supporting the idea that the small number of degrees of freedom observed in the dark matter haloes formed in cosmological N-body simulations (or even in the optical spectra of nearby galaxies, see e.g. Ascasibar & Sánchez Almeida 2011) merely reflects the statistical properties of Gaussian random peaks in the early universe (Ascasibar et al. 2004, 2007). Not only the shapes of $\Psi(\bar{\epsilon})$ on the bottom panels on Figures 1 and 2 are

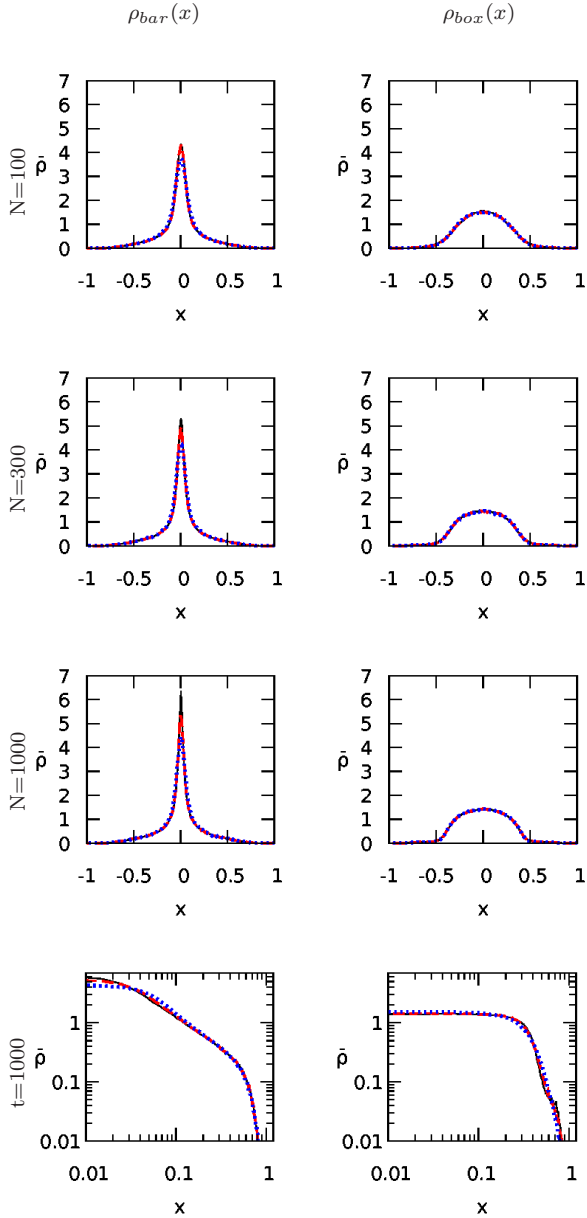


Figure 3. Dependence of the mean density profile $\bar{\rho}(x)$ on time (top three panels) and N (bottom panels), for both the *bar* (left column) and *box* (right column) cases. On the upper panels, results for $t = \{100, 300, 1000\}$ are plotted as dotted blue, dashed red, and solid black lines, respectively. On the bottom panels, these line styles denote $N = \{100, 300, 1000\}$, respectively.

markedly different; the values of $\Psi(x, v)$ on the top panels, as well as the density and velocity distributions plotted in Figures 3 and 4, show that the probability density of the final state in the *bar* case is much more concentrated near the origin of phase space (particles close to the centre, moving at slow velocities) than in the *box* case (see the discussion in the next Section).

Although the evolution of $\Psi(x, v, t)$ seems to be remarkably insensitive to the adopted number of particles, we do detect a mild dependence on N . First and foremost, the dispersion in phase space seems to be slightly faster for low values of N , qualitatively consistent with the idea that the

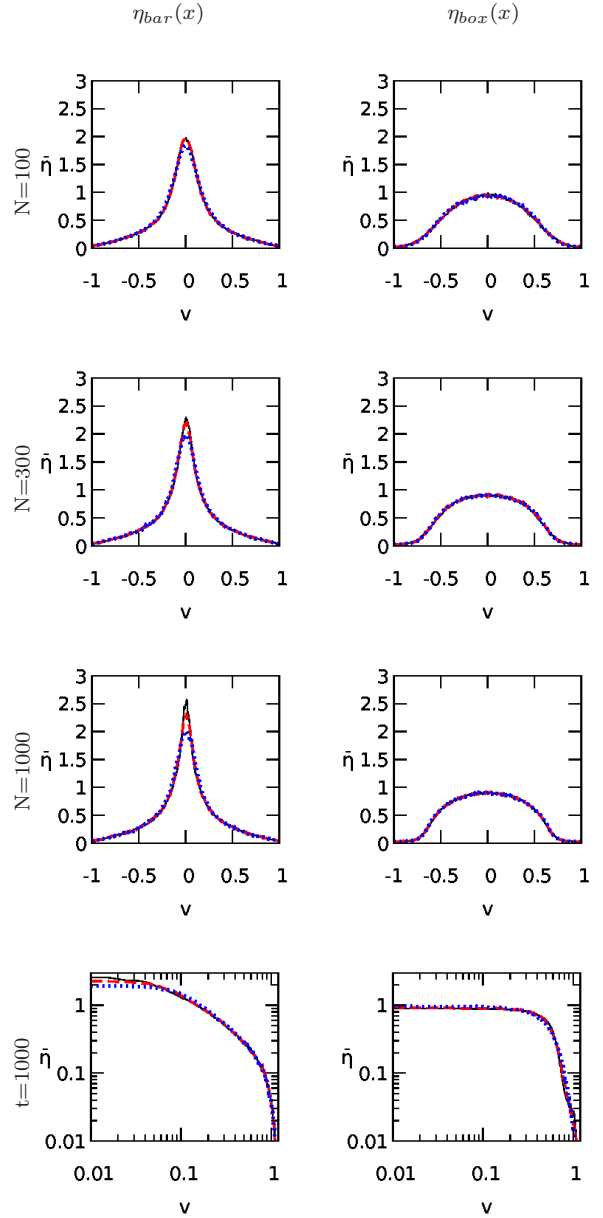


Figure 4. Dependence of the mean velocity distribution $\bar{\eta}(x)$ on t and N . Colours and line styles are identical to those in Figure 3.

amplitude of random fluctuations in the acceleration (10) scales as $\frac{1}{\sqrt{N}}$. This can be seen in the early evolution of $\Psi(x, v, t)$ (the thickness of the distortions at $t = 3$ and $t = 10$ on the top panels of Figures 1 and 2) as well as on the time it takes the system to approach an apparently steady state. Comparing $t = 100, 300$, and 1000 in Figures 3 and 4, we do not observe any relevant change in the density or the velocity distribution of the *box* case beyond $t = 100$ for any value of N , although the phase-space structures (evident as tails on the top panels of Figure 2 and bumps at $\bar{\epsilon} \sim 0.8$ on the bottom panels) survive for a longer time as the number of particles is increased. On the other hand, the *bar* shows no obvious evolution beyond $t = 300$ for $N = 100$, but the maximum values of $\Psi(\bar{\epsilon})$, $\bar{\rho}(x)$, and $\bar{\eta}(v)$ do increase steadily with time for both $N = 300$ and $N = 1000$.

Besides the characteristic time of diffusion, the value of

N also affects the details of the quasi-stationary state. On the one hand, the maxima of $\Psi(\bar{\epsilon})$, $\bar{\rho}(x)$, and $\bar{\eta}(v)$ decrease with the number of particles for the *bar* case. On the other hand, the *box* shows subtle differences in the opposite direction: for $N = 100$, the maximum of Ψ is located at the origin of positions and velocities, but for the other values of N , it occurs along a ring in phase space, roughly corresponding to $\bar{\epsilon} \sim 0.3$ (bottom panel of Figure 2). This translates into $\bar{\rho}(x)$ and $\bar{\eta}(v)$ being slightly steeper for $N = 100$ in Figures 3 and 4.

In order to address the dependence with N over a broader range and shed some light on the possible extrapolation towards $N \rightarrow \infty$, we show in Figure 5 the probability density $\Psi(x, v, t)$ for values of N up to 10^6 (representative, for instance, of the number of stars in a super-massive star cluster or a tiny dwarf galaxy). These data make it clear that even the small differences observed between 100 and 1000 particles are indeed significant, with the most relevant aspect being the slower diffusion in phase space.

It is also noteworthy that diffusion slows down the rotation of the *bar* in phase space. At $t = 6$, only the $N = 10^6$ simulations have reached the maximum expansion state (a horizontal bar), whereas the smaller- N simulations display a thicker configuration at a certain angle with respect to the x axis. At $t = 10$, the system is almost at maximum contraction (a vertical *bar*) for $N = 100$, and there is some delay with respect to the periodic solution of the collisionless Boltzmann equation for $N = 10^6$. In fact, the results for $N = 10^6$ at $t = 10$ are fairly similar to the $N = 1000$ counterpart at $t = 6$ (i.e. one revolution less around the origin).

Comparing the differences between $N = 10^2 - 10^3$ and $N = 10^3 - 10^6$, our results show that the characteristic times for both diffusion and phase lag with respect to the periodic solution of the collisionless Boltzmann equation scale very slowly with the number of particles. Although we caution that logarithmic scaling is far from proven, Figure 5 suggests that three orders of magnitude in N are roughly equivalent to a factor of about two in time.

6 DISCUSSION

The problem of gravitational collapse in one spatial dimension has been widely studied in the literature under the traditional interpretation based on deterministic initial conditions. Particular analytical solutions of the collisionless Boltzmann equation for the distribution function $f(x, v, t)$ have been derived under different assumptions (e.g. Fillmore & Goldreich 1984; Bertschinger 1985; Alard 2013; Colombi 2015), and several attempts have been made to solve it numerically without resorting to the N-body approximation (e.g. Hahn et al. 2013; Yoshikawa et al. 2013; Colombi & Touma 2014; Hahn & Angulo 2016; Mocz & Succi 2017; Sousbie & Colombi 2016). Initial conditions similar to our *bar* and *box* cases have previously been considered, and the reported results are fairly consistent with our findings if we identify the distribution function with the expected average $\bar{f}(x, v, t)$, weighted over all possible realisations of the *random* initial conditions.

6.1 Cold collapse

It is well known, for instance, that cold initial conditions – all particles located along a thin line in phase space with negligible velocity dispersion – yield density profiles that are well described by a power law $\rho(x) \propto x^{-\alpha}$ with logarithmic slope $\alpha \simeq 0.5$ (e.g. Binney 2004), $\alpha \simeq 0.47$ (e.g. Schulz et al. 2013), or $\alpha \simeq 0.4$ (e.g. Colombi & Touma 2014) over a large radial range. All these authors, however, add a sinusoidal velocity perturbation to the bar. Otherwise, they would recover the periodic solution described in Section 2.2, valid both for a continuous fluid as well as for N equispaced particles. We do think that the physical problem of cold collapse is more conveniently formulated under the proposed interpretation: the evolution of N particles starting with strictly null velocity and random uniform position between $x = -\frac{1}{2}$ and $x = \frac{1}{2}$. There is no need for an *ad hoc* velocity perturbation in our approach. Any system with N randomly distributed particles will slowly diffuse out from the initially cold configuration and end up in a quasi-stationary state of the form $\Psi(\bar{\epsilon})$ where $\rho(x)$ is strongly peaked towards the centre.

The precise time scale to approach the quasi-stationary state increases with the number of particles, and it is unclear whether the limit $N \rightarrow \infty$ actually corresponds to the collisionless Boltzmann equation or not (see e.g. the discussion in Colombi & Touma 2014). In any case, physical systems are characterised by a large – yet *finite* – number of particles. Based on the relatively little difference that we observe between the evolution of our test cases for $N = 100$ and $N = 10^6$, we do not expect that increasing N by several orders of magnitude leads to qualitative changes in the overall picture. Regardless of whether $N \rightarrow \infty$ eventually converges towards the collisionless Boltzmann equation, we argue (in contrast to Colombi & Touma 2014) that investigating the dependence with N is the most appropriate avenue to understand the dynamics of real systems (see the discussion at the end of Section 6.4 below).

6.2 Central ‘core’

One of the aspects that is most sensitive to the number of particles in the system is the presence of a ‘core’ (where \bar{f} , $\bar{\rho}$, and $\bar{\eta}$ are constant) sufficiently close to the origin of phase space. Analogous results have been reported in previous studies, based on both N-body simulations with equispaced initial conditions as well as other schemes to solve the Vlasov-Poisson equation. The physical origin of this core is, however, still debated, and several effects that contribute to its appearance have been put forward:

As pointed out by Binney (2004), discreteness prevents an accurate sampling of the ‘true’ continuous distribution function, and the interplay between phase mixing and violent relaxation is ‘prematurely’ terminated. While this is certainly an artefact for $N' \ll N$, it represents a real physical process for the correct value of N , and we propose that determining the extent of the core as a function of particle number could actually provide an estimate of this quantity in astrophysical N-body systems, such as star clusters, galaxies, or even dark matter haloes.

On the other hand, velocity dispersion (e.g. Tremaine & Gunn 1979; Melott 1983; Teles et al. 2011;

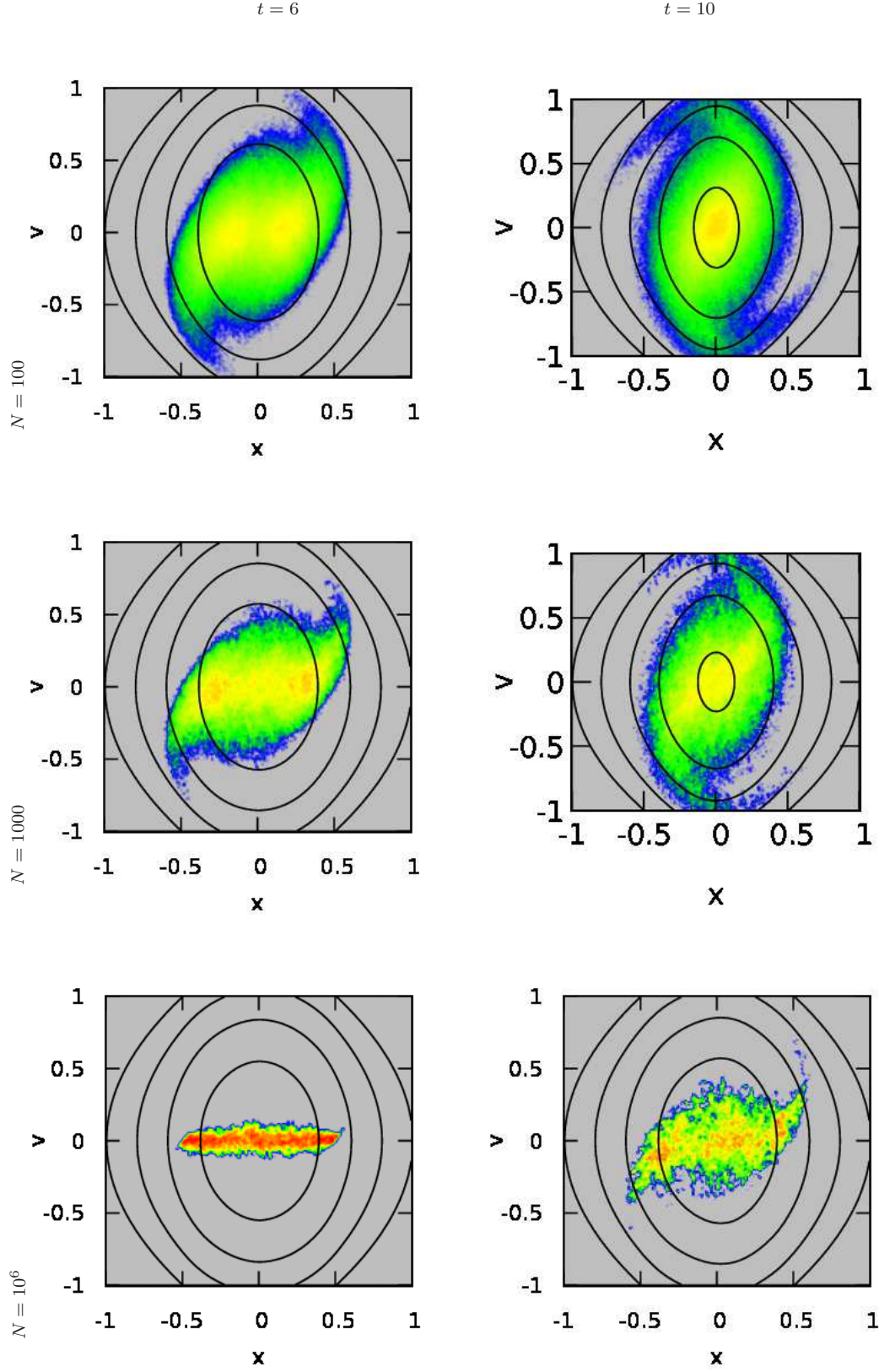


Figure 5. $\Psi(x, v, t)$ in the *bar* case for $t = \{6, 10\}$ and $N = \{100, 1000, 10^6\}$. Colour scale and contour levels are identical to those in Figure 1.

Joyce & Worrakitpoonpon 2011; Colombi & Touma 2014) also leads to the development of a central core, often attributed to the fact that, according to Liouville's theorem, the fine-grained distribution function in phase space cannot increase, and therefore the finite initial value places a strong upper limit at any later time. This is extremely relevant for our *box* case, and Teles et al. (2011) proposed a theoretically-motivated *ansatz* for the analytical form of the quasi-stationary $f(\epsilon)$ consisting on a central value f_0 up to some 'Fermi level' ϵ_0 delimiting the core and another constant value $f_h < f_0$ up to the maximum energy ϵ_h attained by the particles in the outer, diffuse halo. This is broadly consistent with our numerical results, in the sense that the *box* case presents a fairly well-defined core where $\bar{f}(\bar{\epsilon}) \sim 1$ (the initial value), but, rather than a sharp transition to an outer halo, Figure 2 suggest that the system evolves towards a state where \bar{f} is a gradually decreasing function of $\bar{\epsilon}$ in the outer parts, reminiscent of the exponential cut-off predicted by Maxwell-Boltzmann or Lynden-Bell statistics (see e.g. Levin et al. 2014), which is also observed in the *bar* case (cf. Schulz et al. 2013).

Finally, the growth of substructure from initially small fluctuations of a cold state induces a similar effect on the particle distribution in the central regions. As shown by Schulz et al. (2013), adding a short-wavelength perturbation of reduced amplitude to an infinitely thin sheet in phase space breaks the self-similarity of the collapse and the power-law density profile of the final state. Similar results are reported by Colombi & Touma (2014), where the extent of the core depends on both the amount of velocity dispersion as well as on the presence of substructure. The interpretation of the core is in this case far from trivial. According to Schulz et al. (2013), it is due to the impossibility of accurately tracing the phase-space sheet (similar to the discreteness effects advocated by Binney 2004), whereas Colombi & Touma (2014), based on the waterbag method, point out that the constant-density core is actually a rather intricate and chaotic structure in phase space. This structure is difficult to quantify because it does retain detailed memory of the initial conditions, but it is unrelated to discreteness effects, and it should be independent on the number of particles (in particular, it is expected to be present also in the limit $N \rightarrow \infty$).

All the three factors we just outlined (finite probability, discreteness, and small-scale fluctuations) are inherent to our approach. Each individual realisation of the initial condition samples the probability distribution Ψ (which may be, in general, finite over all phase space) with a discrete number N of particles. Random initial conditions introduce a substantial amount of small-scale perturbations (Poisson noise), leading to the formation of numerous substructures and a complex ('chaotic') distribution of particles in phase space. However, the details of such distribution are univocally determined by the particular realisation of the initial conditions, and they wash away after averaging over many independent realisations, eventually yielding a smooth probability distribution at all times. This constitutes an important difference with respect to the traditional approach based on deterministic initial conditions, both for a finite N as well as for a continuous fluid meant to represent $N \rightarrow \infty$.

6.3 Averaging

Averaging is, in fact, a key concept of our approach. From a theoretical point of view, it provides a well-defined and physically-motivated prescription to go from a fine-grained, discrete description of the system, where the distribution function $f(x, v, t)$ is a sum of Dirac deltas, to a probabilistic description in terms of the probability density $\Psi(x, v, t)$ or, equivalently, the *expected* phase-space density $\bar{f}(x, v, t)$, that is most likely continuous and smooth in any realistic system.

In practice, some authors (e.g. Joyce & Worrakitpoonpon 2010; Schulz et al. 2013; Levin et al. 2014) do average over several simulations with slightly different number of equispaced particles and/or over a given time interval in order to reduce noise. The probabilistic interpretation provides not only a rigorous justification for a similar procedure, but, more importantly, ensures that the ensemble of simulations that are averaged are statistically independent and that the true solution is recovered in the limit $S \rightarrow \infty$.

When averaging over a short time interval, adjacent snapshots are certainly correlated; if the time interval is long compared to the dynamical time, correlations will decrease (albeit not vanish), but the evolution of the system may start to play a role. Arguably, the correlation between simulations with slightly different values of N should decay after a sufficiently long time, but a careful analysis should be carried out in order to determine the consequences of averaging over such an ensemble. In both cases, it is clear that it is only possible to average over a limited number S of simulations that cannot be made arbitrarily large.

In the proposed approach, though, different realisations of the initial conditions will remain statistically independent at all times. Since they are all evaluated at exactly the same precise time t , there is no downside to increasing the number of simulations, and the only limit to S is imposed by the available CPU time. In principle, one would expect that statistical fluctuations of $\bar{f}(x, v, t)$ around the true solution should decrease as $S^{-1/2}$.

6.4 Dependence with N

In fact, the number of particles within any of our cells of size $\Delta x \Delta v$ in phase space³ is roughly proportional to the product $N S$. To first order, increasing the number of particles N used in each simulation has a similar effect as increasing the number S of simulations.

From a computational point of view, it is much more advantageous to run additional simulations than to use a larger number of particles, both in terms of memory requirements (a simulation with small N fits in any laptop computer) as well as CPU time. Even if the N-body algorithm scaled as $\mathcal{O}(N)$ – rather than e.g. $\mathcal{O}(N \log N)$ –, communication between different processors, if needed, would impose an overhead with respect to running S independent simulations, which is an embarrassingly parallel problem. Moreover, increasing N yields a much more complex evolution due to the formation of a larger number of substructures on smaller and

³ One may decrease noise and reach a lower measurable density $\bar{\Psi}_{\min} = \frac{1}{\Delta x \Delta v}$ by increasing the cell size, at the expense, of course, of a coarser graining.

smaller scales. In each individual simulation, phase space is better resolved, and the dynamics of the system is *physically* more intricate. The time between particle collisions near the centre of every single substructure becomes very short, and the number of timesteps required to reach a given time t is an increasing function of N .

Moreover, our results show that the evolution towards a quasi-stationary state is faster for systems with small N . Unfortunately, they also indicate that, consistently with the traditional approach, the exact form $\Psi(\bar{\epsilon})$ of such state is found to depend (weakly) on the total number of particles. The difference is mostly restricted to the core discussed in Section 6.2, and it does not seem to affect too much the outer parts. Our results are consistent with Binney (2004) in the sense that discreteness effects may lead to an overestimation of the core size in the cold-collapse (*bar*) case, but we would like to stress once again that this feature is indeed physical in the probabilistic approach, and it will always be present in any real system with finite number of particles. On the other hand, the core size tends to *increase* with N in the warm-collapse (*box*) case. Although much longer simulations would be required in order to test this conjecture, we speculate that collisions (more important at small N) tend to drive the system towards thermal equilibrium, and therefore the solution is closer to the predictions of Maxwell-Boltzmann statistics (flatter than a power law, but more concentrated than constant Ψ).

In any case, understanding the dependence with N is not only an extremely interesting academic question, but it is also of the utmost importance in the context of N -body simulations where $N' \ll N$, both under the traditional and the probabilistic interpretations of the problem. As mentioned above, the relatively small differences between $N = 100$ and $N = 10^6$ hint that the phase-space structure of astrophysical N -body systems might be closer to the results of currently available simulations than to the predictions of the collisionless Boltzmann equation, strictly valid only for a continuous fluid. The details, however, are important. A stellar cluster, for instance, would be an example of a warm system (starting from a turbulent molecular cloud) containing typically less than a million particles (stars), and therefore it is clear that finite- N effects must play a dominant role in its evolution. In contrast, even assuming a fairly heavy dark matter particle, with mass $m_{\text{dm}} c^2 \sim \mathcal{O}(\text{TeV})$, the smallest dark matter halo to host a galaxy would contain of the order of $N \sim \frac{10^8 M_{\odot} c^2}{1 \text{ TeV}} \sim 10^{62}$ particles. In this case, finding the exact time scale for diffusion in phase space is critical in order to gauge whether such system would be better described by the collisionless Boltzmann equation or by following the dynamics of $N' \sim \mathcal{O}(10^6)$ tracers.

7 CONCLUSIONS

In the present work we introduce a new interpretation of the N -body problem, based on the one-point probability density Ψ of finding a particle in a region (x, v) of phase space and the *expected* phase-space density $\bar{f}(x, v, t) = M\Psi(x, v, t)$, where M is the total mass of the system. The difference with the classical approach is both conceptual and practical. On the one hand, our interpretation is intrinsically discrete (the fine-grained distribution function f for any individual

system of N particles is always a sum of Dirac deltas) and probabilistic (we are not interested on the evolution of one of these individual systems, but of a statistical ensemble of realisations of the probability density Ψ at the initial time). Our method is not suitable to study the evolution of a particular deterministic configuration (e.g. the stars in Orion), but of a generic class of systems with a similar distribution in phase space (e.g. stellar clusters of a given size).

On the other hand, the solution to the N -body problem under the proposed interpretation corresponds to an integral over all possible random realisations of the initial conditions. In practice, an arbitrarily good approximation can be obtained by using a finite number S of independent simulations with the same number of particles, where \bar{f} and Ψ can be trivially estimated from the number of particles inside a given bin in (x, v) at time t . At variance with traditional N -body simulations, the accuracy of the numerical solution can be improved by increasing the number of individual realisations. From a computational point of view, our scheme has the additional advantage that increasing S is much more efficient than increasing N in terms of both memory and CPU time.

We have applied our method to two initial probability densities $\Psi(x, v, 0)$: a *bar* in phase space (18), where particles are randomly distributed between $x = -\frac{1}{2}$ and $x = \frac{1}{2}$ with null initial velocity, and a *box* (19) where velocities are also random uniform between $v = -\frac{1}{2}$ and $v = \frac{1}{2}$. Our results show that, analogously to the deterministic interpretation, $\Psi(x, v, t)$ evolves towards a quasi-stationary state that admits a description of the form $\Psi(\bar{\epsilon})$, where $\bar{\epsilon} = \frac{1}{2}v^2 + \phi(x)$ is the energy per unit of mass of a particle located at (x, v) , whose exact form keeps memory of the initial conditions and depends slightly on the number of particles. Most notably, the characteristic time to approach such state is an increasing function of N , and there are subtle changes on the size of the central ‘core’.

We do argue that understanding the dependence with N is of paramount importance to address the validity of using $N' \ll N$ tracers and to discriminate physical effects from numerical artefacts. The traditional interpretation often assumes that the physical evolution of real astrophysical systems is correctly described by the collisionless Boltzmann equation, and study one particular initial configuration (e.g. a certain perturbation of equispaced particles) increasing N as much as possible. Our results suggest that finite- N effects are in general not negligible in any real system; certainly not for $N \leq 10^6$, and probably also for much larger numbers of particles. Studying the evolution of $\Psi(x, v, t)$ as a function of N is in our view a more adequate approach to understanding the N -body problem than focusing on the limit $N \rightarrow \infty$.

ACKNOWLEDGMENTS

Financial support has been provided by projects AYA2013-47742-C4-3-P and AYA2016-79724-C4-1-P (*Ministerio de Economía y Competitividad*; Mineco, Spain), as well as the exchange programme ‘Study of Emission-Line Galaxies with Integral-Field Spectroscopy’ (SELGIFS, FP7-PEOPLE-2013-IRSES-612701), funded by the EU through the IRSES scheme. YA is also supported by the *Ramón y Cajal* programme (RyC-2011-09461; Mineco, Spain).

REFERENCES

- Aarseth S. J., 2003, *Gravitational N-Body Simulations*. Cambridge University Press, Cambridge, UK
- Alard C., 2013, *MNRAS*, **428**, 340
- Ascasibar Y., Sánchez Almeida J., 2011, *MNRAS*, **415**, 2417
- Ascasibar Y., Yepes G., Gottlöber S., Müller V., 2004, *MNRAS*, **352**, 1109
- Ascasibar Y., Hoffman Y., Gottlöber S., 2007, *MNRAS*, **376**, 393
- Barnes J., Hut P., 1986, *Nature*, **324**, 446
- Bertschinger E., 1985, *ApJS*, **58**, 39
- Binney J., 2004, *MNRAS*, **350**, 939
- Binney J., Tremaine S., 2008, *Galactic Dynamics: Second Edition*. Princeton University Press
- Campa A., Dauxois T., Ruffo S., 2009, *Phys. Rep.*, **480**, 57
- Chavanis P.-H., 2013, *A&A*, **556**, A93
- Colombi S., 2015, *MNRAS*, **446**, 2902
- Colombi S., Touma J., 2014, *MNRAS*, **441**, 2414
- Dehnen W., 2000, *ApJ*, **536**, L39
- Dehnen W., 2001, *MNRAS*, **324**, 273
- Fillmore J. A., Goldreich P., 1984, *ApJ*, **281**, 1
- Hahn O., Angulo R. E., 2016, *MNRAS*, **455**, 1115
- Hahn O., Abel T., Kaehler R., 2013, *MNRAS*, **434**, 1171
- Henon M., 1982, *A&A*, **114**, 211
- Hjorth J., Williams L. L. R., 2010, *ApJ*, **722**, 851
- Joyce M., Worrakitpoonpon T., 2010, *Journal of Statistical Mechanics: Theory and Experiment*, **10**, 10012
- Joyce M., Worrakitpoonpon T., 2011, *Phys. Rev. E*, **84**, 011139
- Levin Y., Pakter R., Rizzato F. B., Teles T. N., Benetti F. P. C., 2014, *Phys. Rep.*, **535**, 1
- Lynden-Bell D., 1967, *MNRAS*, **136**, 101
- Melott A. L., 1983, *ApJ*, **264**, 59
- Mocz P., Succi S., 2017, *MNRAS*, **465**, 3154
- Ogorodnikov K. F., 1957, *Soviet Ast.*, **1**, 748
- Plastino A. R., Plastino A., 1993, *Physics Letters A*, **174**, 384
- Rybicki G. B., 1971, *Ap&SS*, **14**, 56
- Schulz A. E., Dehnen W., Jungman G., Tremaine S., 2013, *MNRAS*, **431**, 49
- Shu F. H., 1978, *ApJ*, **225**, 83
- Sousbie T., Colombi S., 2016, *Journal of Computational Physics*, **321**, 644
- Teles T. N., Levin Y., Pakter R., 2011, *MNRAS*, **417**, L21
- Tremaine S., Gunn J. E., 1979, *Physical Review Letters*, **42**, 407
- Wang L., Spurzem R., Aarseth S., Nitadori K., Berczik P., Kouwenhoven M. B. N., Naab T., 2015, *MNRAS*, **450**, 4070
- Yoshikawa K., Yoshida N., Umemura M., 2013, *ApJ*, **762**, 116